Self-Focusing and Stimulated Raman and Brillouin Scattering in Liquids*

Y. R. SHEN† AND Y. J. SHAHAM
Physics Department, University of California, Berkeley, California
(Received 20 April 1967)

Experimental results on the self-focusing of a laser beam in many liquids are reported. It is shown that the optical Kerr effect and electrostriction cannot explain the temperature variation of self-focusing in some liquids. Forward stimulated Brillouin scattering seems important in such cases. Measurements on the generation of stimulated Raman and Brillouin radiation in liquids are presented. The effect of self-focusing and self-trapping on the forward-backward asymmetry in the Stokes generation is discussed. Other qualitative features in the stimulated Raman and Brillouin scattering are explained.

I. INTRODUCTION

WHEN a high-intensity laser pulse traverses a certain distance in a liquid, the beam cross-section often reduces, and in some liquids, thin filaments of extremely high intensity appear. This phenomenon, which is generally known as self-focusing and self-trapping of light beams, has been the subject of intense theoretical[1–7] and experimental[8–18] investigation recently. It is self-focusing and self-trapping that give rise to the many anomalies observed in stimulated Raman and Brillouin scattering in liquids. Physically, self-focusing arises because the refractive index (real part) of the medium increases with the beam intensity (a coherent elastic-scattering process), and because stimulated Brillouin and Rayleigh scattering near the forward direction occur via acoustic and orientational excitations in the medium (a coherent inelastic-scattering process). An alternative way of describing self-focusing is that the width of the beam intensity distribution over its spatial Fourier components increases with distance.

The intensity dependence of refractive indices has been investigated by many authors.[19] In a nonabsorbing medium, it is due to optical Kerr effect, electrostriction, and nonlinear electronic polarizability.[2] For ordinary Q-switched laser intensity, the steady-state refractive index can be written in the form

$$n=n_0+(n_{2\alpha}+n_{2\rho}+n_{2e})\tfrac{1}{2}\,|\,E\,|^2,$$

where E is the laser field strength, and the coefficients $n_{2\alpha}$, $n_{2\rho}$, and n_{2e} are associated with Kerr effect, electrostriction, and nonlinear electronic polarizability, respectively. For most liquids which have been subject to investigation, $n_{2\alpha}$ ranges from 10^{-13} to 10^{-11} esu, while $n_{2\rho}$ is of the order of 10^{-11} esu. In the normal dispersion region, n_{2e} is about 10^{-15} or 10^{-14} esu as estimated from the nonlinear polarizability for third-harmonic generation,[20] and should be negligible compared with $n_{2\alpha}$ and $n_{2\rho}$. It is, however, believed that the Kerr effect gives the dominant contribution to the intensity-dependent part of the refractive index in liquids. The reason is simple. The Kerr effect, arising from molecular reorientation[21] and molecular redistribution,[22] responds almost instantaneously to the Q-switched pulse, but the electrostrictive effect, which involves mass transfer to a region of high beam intensity, cannot follow the rapid intensity variation of the pulse. One can actually show that for a 10^{-8}-sec pulse, the electrostrictive contribution to the refractive index would be negligible

* This research was supported by the Office of Naval Research under Contract No. Nonr-3656(32).
† A. P. Sloan Research Fellow.
[1] G. A. Askar'yan, Zh. Eksperim. i. Teor. Fiz. **42**, 1567 (1962) [English transl.: Soviet Phys.—JETP **15**, 1088 (1962)].
[2] R. Y. Chiao, E. Garmire, and C. H. Townes, Phys. Rev. Letters **13**, 479 (1964).
[3] P. L. Kelley, Phys. Rev. Letters **15**, 1005 (1965).
[4] V. I. Bespalov and V. I. Talanov, JETP Pis'ma v Redaktsiyu **3**, 471 (1966) [English transl.: JETP Letters **3**, 307 1966)].
[5] K. Grob and M. Wagner, Phys. Rev. Letters **17**, 819 (1966).
[6] S. K. Akhmanov, A. P. Sukhorukov, and R. V. Khokhlov, Zh. Eksperim. i Teor. Fiz. **50**, 1537 (1966) [English transl.: Soviet Phys.—JETP. **23**, 1025 (1966)].
[7] Yu. P. Razier, JETP Pis'ma v Redaktsiyu **4**, 286 (1966) [English transl.: JETP Letters **4**, 193 (1966)].
[8] Y. R. Shen and Y. J. Shaham, Phys. Rev. Letters **15**, 1008 (1965).
[9] P. Lallemand and N. Bloembergen, Phys. Rev. Letters **15**, 1010 (1965); **16**, 81 (1966).
[10] G. Hauchecorne and G. Mayer, Compt. Rend. **261**, 4014 (1965).
[11] E. Garmire, R. Y. Chiao, and C. H. Townes, Phys. Rev. Letters **16**, 347 (1966).
[12] N. F. Pilipetskii and A. R. Rustamov, JETP Pis'ma v Redaktsiyu **2**, 88 (1965) [English transl.: JETP Letters **2**, 55 (1965)].
[13] C. C. Wang, Phys. Rev. Letters **16**, 344 (1966).
[14] R. G. Brewer and J. R. Lifsitz, Phys. Letters **23**, 79 (1966).
[15] R. Y. Chiao, M. A. Johnson, S. Krinsky, H. A. Smith, C. H. Townes, and E. Garmire, IEEE J. Quantum Electron. **2**, 467 (1966).
[16] N. Bloembergen, P. Lallemand, and A. Pine, IEEE J. Quantum Electron. **2**, 246 (1966).
[17] D. H. Close, C. R. Guiliano, R. W. Hellwarth, L. D. Hess, F. J. McClung, and W. G. Wagner, IEEE J. Quantum Electron. **2**, 553 (1966).
[18] R. G. Brewer and C. H. Townes, Phys. Rev. Letters **18**, 196 (1967).
[19] P. D. Maker, R. W. Terhune, and C. M. Savage, Phys. Rev. Letters **12**, 612 (1964); F. Gires and G. Mayer, Compt. Rend. **258**, 2039 (1964).
[20] P. D. Maker, R. W. Terhune, and C. M. Savage, in *Proceedings of the Third International Congress on Quantum Electronics*, edited by P. Grivet and N. Bloembergen (Columbia University Press, New York, 1964), p. 1559.
[21] P. Debye, *Marx's Handbuch der Radiologei, VI* (Academisehe Verlagsgeselkchaft, Leipzig, Germany, 1925), Chap. V, p. 768; *Polar Molecules* (Dover Publications, Inc., New York, 1929).
[22] S. Kielich, Mol. Phys. **6**, 49 (1963); R. W. Hellwarth, Phys. Rev. **152**, 156 (1966).

compared with the Kerr effect in most liquids. (See Sec. III for more detail.)

Beam components propagating in the off-axis directions can also grow in intensity through stimulated Brillouin and Rayleigh scattering. This also leads to self-focusing phenomenon. Self-focusing by this mechanism has so far received little attention. In fact, the gain of stimulated Brillouin scattering near the forward direction is rather high even for a short Q-switched pulse. For self-focusing of the laser pulse in liquids with small Kerr constants, stimulated Brillouin scattering could be as important as the Kerr effect. In this paper, we show, from our measurements on the temperature variation of self-focusing action in different liquids, that this is indeed the case. The relative importance of the Kerr effect and stimulated Brillouin scattering to self-focusing can be obtained from these measurements since the Kerr effect is inversely proportional to temperature, but stimulated Brillouin gain increases as temperature increases.

While self-focusing in liquids seems to be qualitatively understood, the dynamics with which a beam, after being self-focused, breaks into self-trapped filaments (known as small-scale trapping[15]) is not yet understood,[6] although the size of the filaments seems to be connected to the Kerr constant of the medium.[15] As one would expect, both self-focusing and self-trapping affect dramatically the nonlinear optical processes in liquids, in particular, stimulated Raman scattering and backward stimulated Brillouin scattering. Self-focusing gives rise to the observed threshold in stimulated Raman and Brillouin scattering,[13] and the presence of intense filaments is responsible for the anomalously high Raman and Brillouin gain above threshold.[8–10] Without knowing the dynamics of filament formation, it is, however, difficult to calculate qualitatively the effect of self-focusing on the stimulated scattering. In this paper, we present some experimental results on first-order Stokes and Brillouin generation, and discuss qualitatively how their characteristics, the forward-backward asymmetry of the Stokes radiation, the temperature effect, etc., are dominated by self-focusing and self-trapping. Experimental results will be shown in Sec. II, followed by discussion in Sec. III.

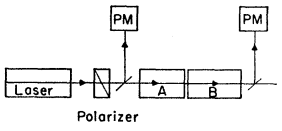

FIG. 1. Experimental set-up of the two-cell method for measuring self-focusing strength of a liquid.

II. EXPERIMENTS

A 3-in. ruby laser, Q-switched by cryptocyanine solution, was used in the experiments. The beam was limited to a diameter of 2 mm. The average peak power of the 15-nsec Q-switched pulses was about 75–100 MW/cm², depending on the cavity parameters. The self-focusing action of the beam in a liquid was investigated by the two-cell scheme.[8] (Figure 1.) Here, the laser beam was passed through two cells in series. They were separated by a distance of 2 cm to allow for windows and a beam splitter when the back-scattered radiation was monitored. The first cell was filled with the liquid under investigation, and the second cell with liquid of low Raman threshold or strong self-focusing action, such as nitrobenzene or carbon disulfide. Self-focusing of the beam in the first cell was then easily detected by the decrease of Raman threshold for liquid in the second cell. To avoid complication, the length of the first cell was always kept below its own Raman threshold. This method has much higher sensitivity than the single-cell method in which the self-focusing action is measured by the observed Raman threshold for liquid in the same cell.[13] It is sensitive in the sense that relatively weak self-focusing action in liquids such as hexane and water can now be measured.[23] One can

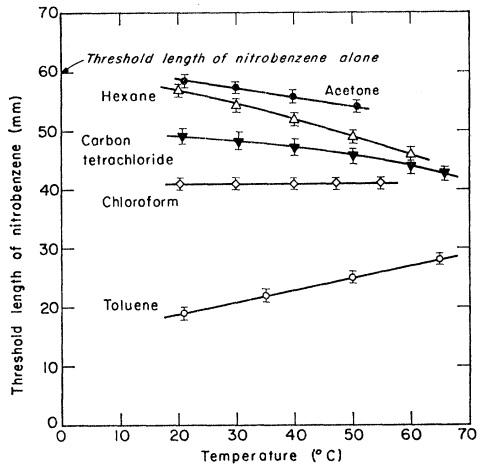

FIG. 2. Temperature variation of self-focusing in different liquids. A longer threshold length of nitrobenzene indicates weaker self-focusing action. See the text.

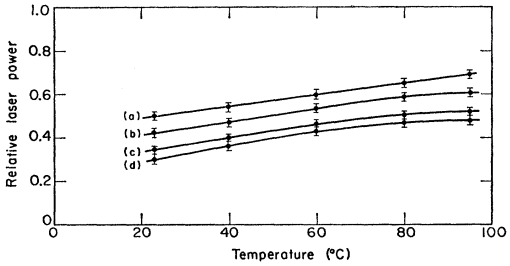

FIG. 3. Effect of a nitrobenzene self-focusing cell on the temperature variation of the Raman threshold of a 15-cm toluene cell. Length of the nitrobenzene cell: (a) 0, (b) 1.3, (c) 2.5, and (d) 5.0 cm.

[23] In liquid with weak self-focusing strength, stimulated Raman and Brillouin scattering may appear before the beam is self-focused to a minimum cross section. Consequently, Raman and Brillouin thresholds of the liquid are no longer a measure of the self-focusing strength. Hexane is a good example.

TABLE I. The relative self-focusing strengths in different liquids measured in terms of the cell length of the liquid which reduces the Raman threshold of 15-cm toluene by 5% when inserted in front of the toluene cell. For nonpolar liquids, $n_{2\alpha}$ are obtained from the dc Kerr constants in Ref. 30. For polar liquids, $n_{2\alpha}$ are either obtained from the experimental values of M. Paillette [Compt. Rend. **262**, 264 (1966)] or from the calculated values of Y. R. Shen [Phys. Letters **20**, 378 (1966)]. g_R is calculated from Eq. (10) with $k_{sx}=2/d$ and $d=0.1$ cm for a 100-MW/cm² ruby-laser beam. g_B is calculated from Eq. (16) with $k_{sx}=2/d$, $d=0.1$ cm, $\Delta\omega=\Gamma$, and $\delta=2\times10^{-8}$ sec for a 100-MW/cm² ruby-laser beam.

	Observed self-focusing strength (in.)	$10^{12}\,n_{2\alpha}$	$10^{2}\,g_R$	$10^{3}\,g_B$	$10^{2}\,(g_R+g_B)$	(g_B/g_R) (%)
Carbon disulfide	$\frac{3}{8}$	11.3	6.8	7.4	7.54	10.9
Nitrobenzene	$\frac{7}{16}$	8.6	6.1	4.1	6.51	6.7
Bromobenzene	1	4.7	4.5	3.0	4.80	6.7
m-xylene	$1\frac{3}{8}$	3.0	3.7	4.8	4.18	13.0
Benzene	$1\frac{3}{4}$	2.3	3.2	5.0	3.70	15.6
Aniline	4	1.1	2.2	4.0	2.60	18.2
Chloroform	5	0.53	1.57	2.6	1.83	16.6
Carbon tetrachloride	$5\frac{1}{2}$	0.33	1.24	2.5	1.49	20.2
Hexane	$5\frac{7}{8}$	0.23	1.06	3.5	1.41	33.0
Acetone	6	0.23	1.07	2.7	1.34	25.2

easily determine the relative self-focusing strength of different liquids using this method. With the laser peak intensity at about 100 MW/cm², we measured the cell lengths of liquids required to reduce the Raman threshold of toluene in the second cell by 5%. The results, together with $n_{2\alpha}$ are given in Table I. Note that the self-focusing strengths of various liquids, except perhaps acetone and hexane, follow the same order as their optical Kerr constants.

The temperature dependence of self-focusing was investigated by varying the temperature of the first cell (15 cm in length). The second cell was filled with nitrobenzene in this case. The results for a few liquids are shown in Fig. 2. It is seen that the self-focusing action in toluene decreases with increase of temperature. This holds for all liquids with large Kerr constants. The temperature variation is similar to that of Raman and Brillouin threshold of liquid in a single cell.[8] This supports the idea that stimulated Raman and Brillouin scattering in these liquids are initiated by strong self-focusing of the beam into hot filaments. However, in acetone, hexane, and carbon tetrachloride, self-focusing gets stronger with increasing temperature, suggesting that besides the Kerr effect, some other mechanism now comes into play. As we shall show in the next section, the contribution of forward stimulated Brillouin scattering to self-focusing is indeed non-negligible in these liquids. The question also arises on whether self-focusing in the first cell would eliminate the temperature dependence of Raman threshold in the second cell. This was tested by using a 15-cm toluene cell with variable temperature proceded by a nitrobenzene focusing cell. As shown in Fig. 3, the temperature variation of Raman threshold in toluene changes only slightly with the focusing cell. The reason is that a major part of self-focusing of the beam actually happens not in the first cell but in the second cell. The filaments have not yet been formed in the first cell. The temperature variation in toluene did nearly vanish when the nitrobenzene cell was above its own threshold, but the results become less meaningful because of the possibility of depletion of laser power by stimulated Raman and backward Brillouin scattering in the nitrobenzene cell.

Wang[13] has shown that for a single cell, the inverse Raman threshold length varies linearly with the square root of the laser power.[3] We found the same result in CS_2 and nitrobenzene at relatively low power level, as shown in Fig. 4. As the laser power increases, the curves start to deviate from the straight line. This suggests that another mechanism for self-focusing may have set in at higher laser intensity.

We are also interested in the generation of stimulated Raman and backward Brillouin scattering in liquid with strong self-focusing properties. A toluene cell was used in the measurements. One of the interesting anomalies resulting from self-focusing and self-trapping is the forward-backward asymmetry in stimulated Raman process. Figure 5 shows the variation of the first-order Stokes power as a function of the cell length at three different laser powers. Note that the forward-backward asymmetry varies with the cell length, although the backward Stokes power is always higher just above

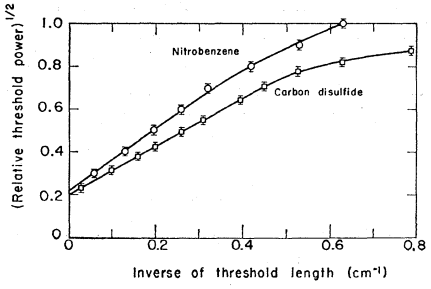

FIG. 4. Variation of the square root of Raman threshold power as a function of inverse of the cell length in CS_2 and nitrobenzene.

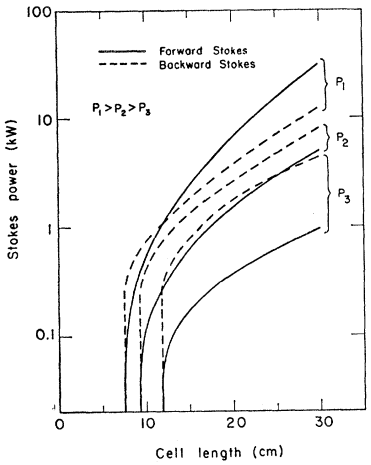

FIG. 5. First-order forward and backward Stokes power versus the cell length at three laser powers, $P_1=80$, $P_2=67$, and $P_3=53$ MW/cm².

threshold. The forward Stokes becomes more intense at long cell lengths. Care was taken to insure that the asymmetry was not induced by reflection from windows. In Fig. 6, the variarion of Stokes power, generated from a 20-cm toluene cell, as a function of laser power is given. The set of curves on the left corresponds to the case where a 2.5-cm nitrobenzene cell was inserted in front of the toluene cell. As expected, the curves look similar to those of Fig. 5. The variation of backward Brillouin power with laser power is also incorporated in Fig. 6.

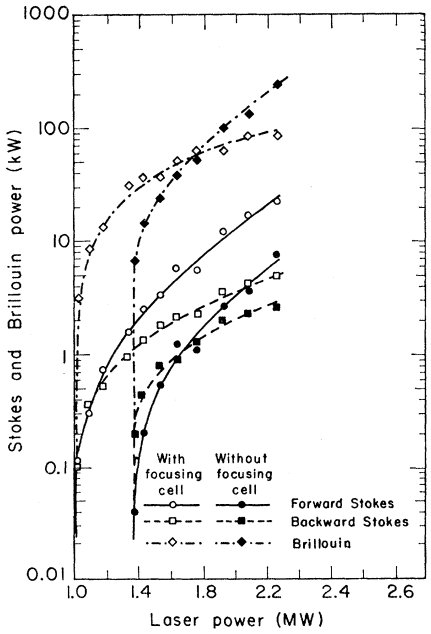

FIG. 6. Variation of Stokes and Brillouin power generated in a 20-cm toluene cell as a function of laser power, with and without a 2.5-cm nitrobenzene self-focusing cell.

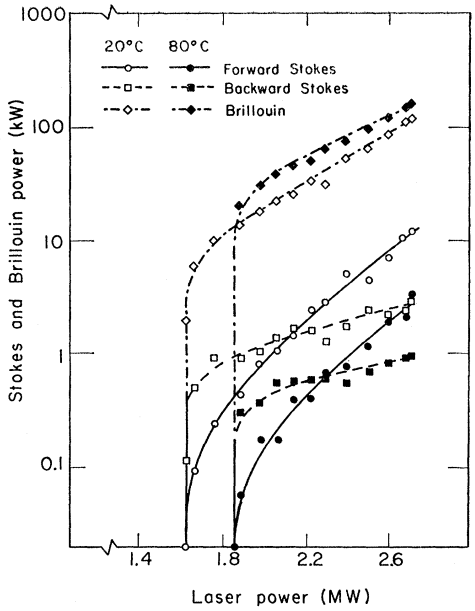

FIG. 7. Variation of Stokes and Brillouin power with laser power in 15-cm toluene at two different temperatures.

Figures 7 and 8 give the variation of Stokes and backward Brillouin power with the laser power in toluene and hexane, respectively, at two different temperatures. It is seen that at the higher temperature, the Raman and Brillouin threshold for toluene is higher, but as the laser power increases, the Brillouin radiation finally becomes more intense than the one at the lower temperature. In hexane, the Brillouin radiation has lower threshold and higher power at the higher temperature. No stimulated Raman radiation from hexane was observed.

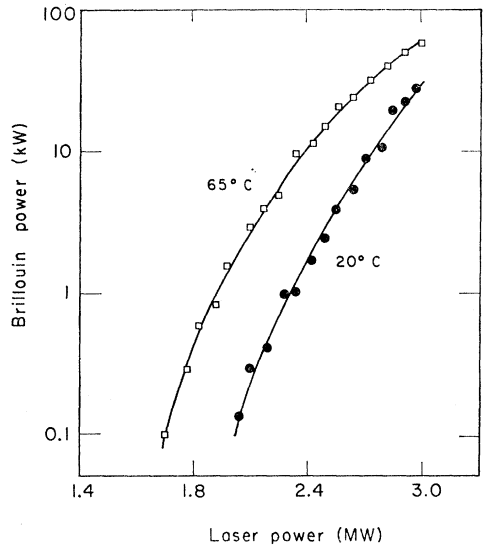

FIG. 8. Variation of Brillouin power with laser power in 15-cm hexane at two different temperatures.

The above measurements of intensities were made by using silicon photodiodes and a Tektronix 555 oscilloscope. The intensity values correspond to the peak values of the integrated pulses. The temporal structure of the generated Stokes and backward Brillouin radiation was investigated by using an FW-114 photodiode and a Tektronix 519 oscilloscope. Both the forward and the backward Stokes radiation from toluene were composed of short pulses of about 10^{-9} sec long, in partial agreement with observations of other workers.[18,24] The Brillouin radiation also contained short pulses, somewhat similar to what was observed by Maier *et al.*,[25] but they are not as sharp as the pulses in the Stokes radiation. Near threshold, both Stokes and Brillouin radiation consists of a single short pulse. Because of the short cells we used in our experiments, the depletion of total laser power in the Raman and Brillouin generation was not nearly as much as in the case of Maier *et al.*[25]

III. CALCULATION AND DISCUSSION

Generally speaking, self-focusing arises as a result of interaction of the light beam with the density variation and molecular reorientation and redistribution in the medium. The propagation of the light beam in liquid is described by the wave equation

$$\left(-\nabla^2+\frac{\epsilon}{c^2}\frac{\partial^2}{\partial t^2}\right)\mathbf{E}(\mathbf{r},t)=-\frac{4\pi}{c^2}\frac{\partial^2}{\partial t^2}\mathbf{P}^{\mathrm{NL}}(\mathbf{r},t). \quad (1)$$

In this case, the polarization of the medium can be written as

$$\mathbf{P}=\chi,\mathbf{E}(\mathbf{r},t),$$
$$\chi=\sum_{m=1,2,\ldots}\rho^m\alpha_m, \quad (2)$$

where terms with $m>1$ arise because of correlation between molecules.[21] The nonlinear polarization P^{NL} appears as a result of change in ρ and α_m induced by the light fields.

$$\mathbf{P}^{\mathrm{NL}}(\mathbf{r},t)=\left[(\partial\chi/\partial\rho)\Delta\rho(\mathbf{r},t)+\sum_m(\partial\chi/\partial\alpha_m)\Delta\alpha_m(\mathbf{r},t)\right]\mathbf{E}(\mathbf{r},t). \quad (3)$$

The density variation $\Delta\rho$ obeys the acoustic wave equation

$$\left(-\nabla^2+\frac{1}{v^2}\frac{\partial^2}{\partial t^2}-\frac{2\Gamma}{v^2}\frac{\partial}{\partial t}\right)\Delta\rho(\mathbf{r},t)=-\frac{\gamma}{8\pi v^2}\nabla^2\mid E\mid^2(\mathbf{r},t). \quad (4)$$

Here, $v=(1/\rho\beta)^{1/2}$ is the acoustic velocity, β is the isothermal compressibility, Γ is the acoustic damping, γ is defined as $\gamma=\rho(\partial\epsilon/\partial\rho)$, and $\mid E\mid^2(\mathbf{r},t)$ is the slowly varying part of $E^2(\mathbf{r},t)$. The change $\Delta\alpha_1$, reflecting variation in the orientational distribution, is governed by the equation[21]

$$(\partial/\partial t+1/\tau)\Delta\alpha_1(\mathbf{r},t)=(A/\tau)\mid E\mid^2(\mathbf{r},t), \quad (5)$$

where A is a constant inversely proportional to temperature, and τ is the orientational relaxation time. Similar equations probably govern $\Delta\alpha_m$ which are changes induced by molecular redistribution. The relaxation time for molecular reorientation and redistribution is usually rather short ($\sim5\times10^{-11}$ sec).[26] If we limit ourselves to the low-frequency variation of $E^2(\mathbf{r},t)$,[27] then $\Delta\alpha_m(\mathbf{r},t)$ would respond almost instantaneously to $\mid E\mid^2(\mathbf{r},t)$. To the first order, we can write

$$\sum_m(\partial\chi/\partial\alpha_m)\Delta\alpha_m=(n/2\pi)n_{2\alpha}\tfrac{1}{2}\mid E\mid^2(\mathbf{r},t). \quad (6)$$

Self-focusing should therefore be described by the solution of Eqs. (1), (3), (4), and (6). If both $\Delta\rho$ and $\mid E\mid^2$ are Fourier-analyzed, then each Fourier component of $\Delta\rho$ consists of two parts. The part in phase with the driving component leads to change in the (real) refractive index: This is known as electrostriction. The part 90° out of phase with the driving component leads to stimulated Brillouin scattering. From Eq. (4), we find that the electrostrictive part is given approximately by

$$\Delta\rho_e(\mathbf{r},t)=\int d^3r'\left(\frac{-\gamma}{8\pi v^2}\right)\nabla^2\mid E\mid^2\left(\mathbf{r}',t-\frac{\mid\mathbf{r}-\mathbf{r}'\mid}{v}\right)\Big/4\pi\mid\mathbf{r}-\mathbf{r}'\mid. \quad (7)$$

It can easily be shown that for a Gaussian beam of radius r_0 and pulse duration δ, the first-order solution of Eq. (7) with $v\delta\ll r_0$ yields at the peak of the laser pulse,

$$(\partial\chi/\partial\rho)\Delta\rho\approx(nv^2\delta^2/4\pi r_0^2)n_{2\rho}\mid E\mid^2, \quad (8)$$

where

$$n_{2\rho}=\gamma^2\beta/8\pi n.$$

This is because the spatial density variation cannot follow the rapid change in the laser intensity, so that the $-\nabla^2$ term is small compared with the $\partial^2/\partial t^2$ term in Eq. (4). For liquids under investigation, $n_{2\rho}$ is about 1 to 10 times $n_{2\alpha}$. With $v\approx10^5$ cm/sec, $\delta\approx10^{-8}$ sec, and $r_0\approx0.1$ cm, one sees immediately from Eqs. (6) and (8) that the electrostrictive effect is negligible compared with the Kerr effect, and hence is not responsible for the temperature variation of self-focusing in liquids.

Even if the electrostrictive effect is neglected, it is still difficult to find an analytical solution from the

[24] M. Maier, W. Kaiser, and J. A. Giordmaine, Phys. Rev. Letters **17**, 1275 (1966).
[25] M. Maier, W. Rother, and W. Kaiser, Appl. Phys. Letters **10**, 80 (1967).
[26] C. W. Cho, N. D. Foltz, D. H. Rank, and T. A. Wiggins, Phys. Rev. Letters **18**, 107 (1967).
[27] Stimulated Rayleigh scattering with a large frequency shift may be less important for self-focusing, since it is essentially initiated at the noise level.

above equations to describe self-focusing. However, as we mentioned earlier, self-focusing can be described by the amplification of Fourier components propagating in the off-axis direction.

Let us assume a plane wave

$$\mathbf{E}_0=\tfrac{1}{2}\mathcal{E}_0\exp[i\mathbf{k}_0\cdot\mathbf{r}-i\omega_0 t] \tag{9}$$

as the pump field propagating in the medium along the z direction. We are interested in the amplification of a weak wave E_s with wave vector $\mathbf{k}_s$ and frequency ω_s. Bespalov and Talanov[4] and Chiao *et al.*[28] show that the change of refractive index (essentially due to Kerr effect) actually induces an exponential gain for the amplification of E_s.

$$g_R=k_{sx}[-(k_{sx}/k_0)^2+2(n_2/n_0)\mathcal{E}_0^2]^{1/2}, \tag{10}$$

assuming $(\omega_0-\omega_s)\ll 1/\tau$. It turns out that the e-folding length for the growth of E_s with $k_{sx}=2/d$ is just the self-focusing distance z_{foc} of a beam with a diameter d, if $(k_{sx}/k_0)^2\ll 2(n_2/n_0)\mathcal{E}_0^2$.[28]

$$z_{foc}=d/2[2(n_2/n_0)\mathcal{E}_0^2]^{-1/2}. \tag{11}$$

The optimum gain is

$$(g_R)_{opt}=k_0(n_2/n_0)\mathcal{E}_0^2 \tag{12}$$

which occurs at $(k_{sx})_{opt}=k_0[(n_2/n_0)\mathcal{E}_0^2]^{1/2}$. As $\mathcal{E}_0^2$ increases, $(g_R)_{opt}$ would finally become much larger than the gain at $k_{sx}=2/d$. Then, one may find that in a distance less than z_{foc}, the wave E_s with $(k_{sx})_{opt}$ becomes stronger than E_s with $k_{sx}=2/d$, although initially the former is much weaker than the latter. The actual self-focusing distance would then become smaller than z_{foc},[4] and would depend on $\mathcal{E}_0^{-2n}$ with $\frac{1}{2}<n<1$. This is likely to happen in liquids with large Kerr constants. As an example, we have $n_2=1.13\times10^{-11}$ for CS_2. For a 100-MW/cm^2 beam with $d=0.1$ cm, and $\mathcal{E}_0^2=8\times10^5$ esu, we find $(g_R)_{opt}=0.92$ and $(g_R)_{k_{sx}=2/d}=0.067$. This probably explains why in Fig. 4 the inverse of the self-focusing distance depends on the laser intensity as $P^n\propto\mathcal{E}_0^{2n}$ with $n>\frac{1}{2}$ at high intensity. For liquids with small Kerr constants, $(g_R)_{opt}$ is not very different from $(g_R)_{k_{sx}=2/d}$ even at an intensity of 100 MW/cm^2.

The weak wave E_s can also be amplified through forward stimulated Brillouin scattering, governed by the coupled equations

$$\begin{aligned}&(-\nabla^2-\omega_s^2\epsilon_s/c^2)E_s=(4\pi\omega_s^2/c^2)(\gamma/4\pi\rho)E_0\Delta\rho^*,\\&(-\nabla^2-\omega_{ac}^2/v^2-i2\omega_{ac}\Gamma/v^2)\Delta\rho^*=-(\gamma/8\pi v^2)\nabla^2(E_0^*E_s),\end{aligned} \tag{13}$$

with $\omega_s+\omega_{ac}=\omega_0$. For scattering in the near-forward direction, $\mathbf{k}_s+\mathbf{k}_{ac}=\mathbf{k}_0$, the Brillouin power gain is[29]

$$g_B=(k_s\Gamma/vk_{ac})+[(k_s\Gamma/vk_{ac})^2+(\omega_s^2\gamma^2\beta\mathcal{E}_0^2/32\pi c^2)]^{1/2}. \tag{14}$$

Ordinary liquids have $\gamma\sim1$ and $\beta\sim10^{-10}$. Therefore, at the same laser intensity, g_B would be much greater than g_R, if the laser beam were continuous.

In practice, however, the Q-switched laser generates a short pulse of pulse width δ. The amplification of E_s due to Kerr effect is still given by Eq. (10) with $\mathcal{E}_0^2$ replaced by $\mathcal{E}_0^2(t)$, since the response of Kerr effect to $\mathcal{E}_0^2(t)$ is almost instantaneous. The Brillouin gain, on the other hand, is greatly reduced. To estimate the reduction, let us assume that $\mathbf{E}_0$ and $\mathbf{E}_s$ are infinite plane waves which can be represented by

$$\mathbf{E}_0=\mathbf{A}_0\Delta\omega\sum_{m=-N/2}^{N/2}\exp[i(\omega_0+m\Delta\omega)(n_0\hat{k}_0\cdot\mathbf{r}/c-t)], \tag{15}$$

$$\mathbf{E}_s=\sum_{m=-N/2}^{N/2}A_{sm}(z)\Delta\omega\exp[i(\omega_s+m\Delta\omega)(n_s\hat{k}_s\cdot\mathbf{r}/c-t)],$$

where $N\Delta\omega=1/\delta$ and $A_0\Delta\omega=(\mathcal{E}_0)_{max}/N$. Then, the driving term for $\Delta\rho$ in Eq. (13) with wave vector $\mathbf{k}_{ac}=(\omega_0n_0k_0-\omega_sn_s\hat{k}_s)/c$ and frequency $\omega_{ac}=\omega_0-\omega_s$ is

$$+(\gamma^2/8\pi v^2)k_{ac}^2\sum_{m=-N/2}^{N/2}A_0A_{sm}(\Delta\omega)^2\exp[i\mathbf{k}_{ac}\cdot\mathbf{r}-i\omega_{ac}t]$$

for sufficiently large $\Delta\omega$. The coupling of $\Delta\rho$ with the N frequency modes A_{sm} of E_s leads to $(N+1)$ coupled equations, whose solution is of the form

$$A_{sm}(z)=\sum_i C_i\exp(g_iz),$$

where g_i are the eigenvalues. The maximum g_i gives the reduced Brillouin gain, which can be shown to be

$$\begin{aligned}g_B&=-(k_s\Gamma/vk_{ac})+[(k_s\Gamma/vk_{ac})^2\\&\qquad+(\omega_s^2\gamma^2\beta\delta\Delta\omega/32\pi c^2)\mathcal{E}_{0max}^2]^{1/2}\\&\simeq(\omega_s^2\gamma^2\beta vk_{ac}\delta\Delta\omega/64\pi c^2k_s\Gamma)\mathcal{E}_{0max}^2.\end{aligned} \tag{16}$$

This gain would remain roughly unchanged for a beam of finite cross-section ($d\gg\lambda$). Obviously, for $g_B\lesssim\Gamma/v$, we should take $\Delta\omega\sim\Gamma$. Then, with a 100-MW/cm^2 laser beam of $d=0.1$ cm and $\delta=2\times10^{-8}$ sec, the Brillouin gain at $k_{sx}=2/d$ in CS_2 ($\gamma=2.2$, $\beta=0.92\times10^{-10}$) is $g_B\sim4.6\times10^{-3}$. This gain is small compared with the gain g_R due to Kerr effect in CS_2, but in media with small Kerr constants, it can be important. We believe that this forward-stimulated Brillouin scattering is responsible for the temperature dependence of self-focusing in chloroform, CCl_4, hexane, and acetone as shown in Fig. 2.

[28] R. Y. Chiao, P. L. Kelley, and E. Garmire, Phys. Rev. Letters **17**, 1158 (1966).

[29] Y. R. Shen and N. Bloembergen, Phys. Rev. **137**, A1787 (1965). Here, the solution is actually valid only for scattering at a sufficiently large angle such that $k_{ac}/k_s\gg g_B/k_{ac}$.

Since the total gain for E_s is $g \approx g_R + g_B$, the temperature dependence of g at $k_{sx}=2/d$ is

$$dg/dT \simeq -g_R/2T + g_B d\beta/\beta dT, \tag{17}$$

assuming that the temperature dependence of quantities other than $n_{2\alpha}$ and β in g can be neglected. Figure 2 shows $dg/dT=0$ for chloroform at about 100 MW/cm². With $g_R=1.57\times10^{-2}$ and $d\beta/\beta dT=0.01$ [30] for chloroform at $T=300°$K, we should have $g_B=2.62\times10^{-3}$. Equation (16) with $\gamma=1.27$, and $\beta=10^{-10}$ for chloroform gives $g_B=1.7\times10^{-3}$. In Table I, we calculated g_R and g_B at $k_{sx}=2/d$ for various liquids, using the experimental g_B for chloroform as reference and assuming the same dependence of g_B on γ, β and n (Ref. 30) as in Eq. (16). Then, with Eq. (17), one can easily show that for CCl_4, hexane, and acetone, $dg/dT>0$, and for other liquids in the table besides chloroform, $dg/dT<0$ in agreement with our observation.

Experiments on stimulated Raman scattering in liquids show many anomalous effects,[31] such as the anomalous gain,[32] spectral broadening,[9] class-II anti-Stokes radiation,[33] etc. Most of the anomalous effects can now be explained by self-focusing and self-trapping. Nevertheless, the anomalous forward-backward asymmetry in the Stokes radiation has not yet received a satisfactory explanation, although it is believed that this must also be a consequence of self-focusing and self-trapping.

In the self-trapped region essentially all the Stokes radiation is generated in the self-trapped filaments. Assume that individual filaments are isolated from the surrounding, and the Stokes generation in each filament can be described by the steady-state equations[34]:

$$\begin{aligned}
\partial N_{sF}/\partial z &= \sigma N_l(N_{sF}+1),\\
\partial N_{sB}/\partial z &= -\sigma N_l(N_{sB}+1),\\
\partial N_l/\partial z &= -\sigma(N_l N_{sF}+N_l N_{sB}),
\end{aligned} \tag{18}$$

with $N_{sF}(0)=N_{sB}(L)=0$, where $N_l(z)$, $N_{sF}(z)$, and $N_{sB}(z)$ are the average photon numbers per unit length for laser, forward, and backward Stokes fields, respectively, and σ is the scattering coefficient. Then, the solution of Eq. (18) is

$$\begin{aligned}
N_{sF}(L) &= N_{sB}(0)\\
&= \exp\left[\int_0^L \sigma N_l(z)\,dz\right]-1
\end{aligned} \tag{19}$$

which shows that the forward-backward symmetry in the Stokes generation would persist.

The observed forward-backward asymmetry suggests that the filaments are not isolated. The Stokes radiation generated elsewhere in the medium is expected to self-focus together with the laser beam into the self-trapped filaments. Generally, this would increase the rate of forward Stokes generation in the filaments. In fact, the Stokes generation in the filaments is perhaps a transient rather than a steady-state phenomenon. As we mentioned earlier, the Stokes radiation appears as a series of sharp pulses. It was suggested that each filament lasts not much longer than 10^{-10} sec.[18] The Stokes generation in a filament is therefore described by

$$\begin{aligned}
(\partial/\partial z + n_l\partial/c\partial t)N_l &= -\sigma N_l(N_{sF}+N_{sB}),\\
(\partial/\partial z + n_s\partial/c\partial t)N_{sF} &= \sigma N_l(N_{sF}+1),\\
(\partial/\partial z - n_s\partial/c\partial t)N_{sB} &= -\sigma N_l(N_{sB}+1),
\end{aligned} \tag{20}$$

neglecting other nonlinear processes in the filament. The solution of Eq. (20) is difficult, but it can be shown that when the laser peak power is highly depleted in the Stokes generation, and $N_{sF}(z=0)$ is not too much larger than $N_{sB}(z=L)$, where L is the length of the filament, the peak intensity of N_{sB} can be many times higher than that of N_{sF}.[24] This would then enhance the backward Stokes radiation. Of course, the reverse will be true if $N_{sF}(z=0)$ is sufficiently larger than $N_{sB}(z=L)$. Because of our lack of knowledge on how the self-trapped filaments are formed, and because of other nonlinear processes in the filaments, it is quite impossible to describe the analytical details of stimulated Raman scattering in liquids. However, on the basis of what we have just discussed, we can explain qualitatively the observed forward-backward Stokes asymmetry (Fig. 5). After the laser traverses a distance z_f (the self-focusing length) in the liquid, filaments start to show up. The average number of filaments $W(z)$ increases with distance z rapidly, say

$$W(z) = \exp[f(z-z_f)]$$

and the laser input into individual filaments is nearly a constant depending only on the properties of the liquid. Because of self-focusing of Stokes radiation, we would expect that $N_{sF}(z=z_0)>N_{sB}(z=z_0+L)$ for a filament initiated at z_0, and that $N_{sF}(z=z_0)$ increases with z_0 and the laser intensity in the nontrapped region. Thus, when the cell length is increased above z_f, both forward and backward Stokes radiation begin to be generated in the filaments with extremely high gain before saturation in the Stokes generation sets in. This appears as a sharp threshold for the stimulated scattering. After saturation sets in, the backward Stokes radiation would become more intense than the forward as a result of transients, if $N_{sF}(z=z_0)$ is not too much

[30] *International Critical Tables, National Research Council*, (McGraw-Hill Book Co., New York, 1930). *Handbook of Chemistry*, edited by N. A. Lange (Handbook Publishers, Inc., Sandusky, Ohio, 1956).
[31] See, for example, B. P. Stoicheff, Phys. Letters **7**, 186 (1963).
[32] F. J. McClung, W. G. Wagner, and D. Weiner, Phys. Rev. Letters **15**, 96 (1965).
[33] E. Garmire, Phys. Letters **17**, 251 (1965).
[34] R. W. Hellwarth, Phys. Rev. **130**, 1850 (1963).

larger than $N_{sB}(z=z_0+L)$. As the cell length is increased further, more filaments show up, and the increase of $N_{sF}(z=z_0)$ with z_0 enhances the forward Stokes generation in these filaments. The Stokes intensity in the forward direction now grows faster than in the backward direction. Eventually, for a sufficiently long cell, the forward Stokes radiation will become more intense than the backward Stokes, although the reverse is true near the threshold. This explains the crossover of the forward and the backward Stokes curves in Fig. 5.[35] Since $N_{sF}(z=z_0)$ also increases with the intensity of the laser beam, the crossover would appear closer to the threshold length for higher laser intensity as we have observed. A similar argument explains the qualitative behavior of the Stokes curves in Figs. 6 and 7, if we remember that the self-focusing distance z_f in toluene is nearly proportional to the square root of laser intensity.[3] In Fig. 6, the nitrobenzene focusing cell helps the self-focusing action in toluene, enhances slightly the forward Stokes intensity with respect to the backward Stokes, and hence brings the crossover point closer to threshold. Since most of the Stokes amplification comes from the self-trapped region,[36] the slight change in the threshold would not affect greatly the Stokes generation above threshold. The two sets of Stokes curves, with and without the focusing cell, look very much alike except that one is shifted from the other. The Stokes curves in Fig. 7, however, seem to indicate the fact that the Stokes amplification is greater at lower temperature because of a smaller Raman linewidth.

The sharp rise of the Brillouin curves near Raman threshold in Figs. 6 and 7 show that the stimulated Brillouin scattering in toluene is also initiated by the appearance of self-trapped filaments. Nevertheless, since the lifetime of the filaments is short, the Brillouin generation in these filaments is greatly reduced. Thus, relatively, the Brillouin amplification in the nontrapped region is much more important than in the Stokes case. It has a steady-state gain of 0.7 cm^{-1} for a 100 MW/cm^2 laser beam.[37] This large gain is presumably responsible for the higher Brillouin intensity than the Stokes. The Brillouin amplification in the nontrapped region could explain the cross over of the two Brillouin curves in Fig. 6 with and without a focusing cell. At sufficiently high laser intensity, the Brillouin amplification in the nontrapped region would dominate over the Brillouin generation in the filaments. Since the Brillouin amplification depends positively on the isothermal compressibility β, which increases sharply with temperature, the Brillouin intensity is expected to be higher at higher temperature, just as shown in Fig. 7, although the threshold in toluene at higher temperature is higher. In hexane, there is no evidence of the presence of filaments. The Brillouin curves in Fig. 8 also give no indication of sharp threshold. It is believed that in hexane the effect of self-focusing and self-trapping on stimulated Brillouin scattering should be negligible. Then, since the Brillouin amplification increases with temperature, the Brillouin radiation should have higher intensity and hence a lower apparent threshold at higher temperature, as shown in Fig. 8.

IV. CONCLUSION

In most organic liquids, the optical Kerr effect is the dominant mechanism for self-focusing. However, the Kerr effect fails to explain the fact that the self-focusing strength increases with temperature in liquids such as CCl_4, hexane and acetone. For a Q-switched laser pulse, the electrostrictive contribution to self-focusing is often negligible. It is concluded that forward stimulated Brillouin scattering should be responsible for the temperature effect in these liquids. Self-focusing and self-trapping affect drastically the stimulated Raman and Brillouin scattering in liquids. The increase of number of self-trapped filaments with cell length and laser intensity, together with self-focusing and transient effects, explains qualitatively the observed forward-backward asymmetry in the Stokes generation. Other qualitative features in the stimulated Raman and Brillouin scattering can also be explained.

[35] The qualitative features of Fig. 5 can be obtained if we assume that the Stokes radiation generated in each filament is approximated by

$$\left.\begin{aligned} N_{sF}(z_0+L) &= N_{sF}(z_0)\exp(gL) \\ N_{sB}(z_0) &= N_{sB}(z_0+L)\exp(g'L) \end{aligned}\right\}, \qquad 0\leq L\leq L_{sat}$$

$$N_{sF}(z_0+L) = N_{sF}(z_0)N_{l0}/[N_{sF}(z_0)+fN_{sB}(z_0+L)],$$

$$N_{sB}(z_0) = C,$$

$$L_{sat} = (1/g)\ \ln\{N_{l0}/[N_{sF}(z_0)+fN_{sB}(z_0+L)]\},$$

$$g' = (1/L_{sat})\ \ln[C/N_{sB}(z_0+L)],$$

and $N_{sF}(z_0)$, $N_{sB}(z_0+L)$, g, f, and C are numerical constants properly chosen.

[36] The Stokes gain in the nontrapped region is only about 0.25 cm^{-1} even for a 100 MW/cm^2 laser beam. See Ref. 29.

[37] See Ref. 29. The acoustic damping used to calculate the gain is taken from R. Y. Chiao and P. A. Fluery, in *Proceedings of Conference on Physics of Quantum Electronics, Puerto Rico, 1965*, edited by P. L. Kelley, *et al.* (McGraw-Hill Book Co., New York, 1966), p. 241.